

AST 851 Dynamic Meteorology

Department of Physics
Department of Energy & Environ Systems
NC A&T State University

Dr. Yuh-Lang Lin

ylin@ncat.edu
<http://mesolab.org>

5.4 Potential Vorticity

- Claim: For an adiabatic flow, C_a is conserved.

Proof: It has been proved earlier that for an adiabatic flow, θ is conserved. That is, θ is constant following the motion. In addition, ρ is a function of p alone in an adiabatic flow,

$$\rho = \left(\frac{p_o^{R/c_p}}{R\theta} \right) p^{c_v/c_p}$$

Therefore, the circulation theorem becomes

$$\begin{aligned} \frac{DC_a}{Dt} &= -\oint \frac{dp}{\rho} = -\oint \left(\frac{R\theta}{p_o^{R/c_p}} \right) p^{-c_v/c_p} dp \\ &= -\left(\frac{R\theta}{(1-c_v/c_p)p_o^{R/c_p}} \right) \oint d(p^{1-c_v/c_p}) = 0 \end{aligned}$$

\oint (exact differential) = 0

Thus, C_a is conserved following an adiabatic flow.

Using Holton's Eq. (4.4),

$$C_a = C + 2\Omega A_e = C + 2\Omega A \sin \bar{\phi} \quad (4.4)$$

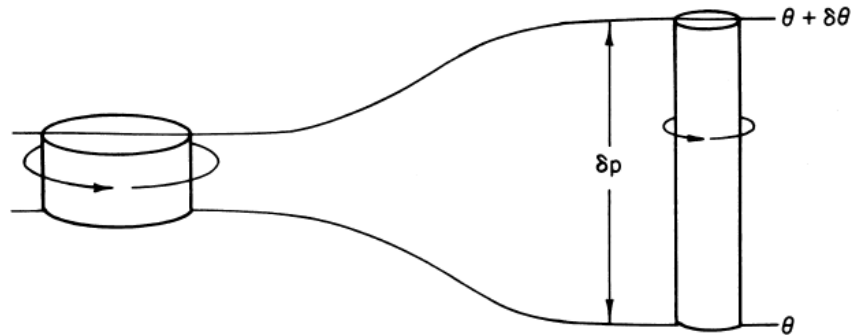
the conservation of C_a following an adiabatic flow can also be rewritten as

$$\frac{DC_a}{Dt} = \frac{D}{Dt} \left(\underbrace{C}_{\text{relative circulation}} + \underbrace{2\Omega A \sin \bar{\phi}}_{\text{planetary circulation}} \right) = \frac{D}{Dt} (C + fA) = 0. \quad (4.10)$$

Recap: The example of negative vorticity generated when moving a non-circulating air to the North Pole **now can be proved!**

- Applying (4.10) to an air column confined between θ_o and $\theta_o + \delta\theta$.

Fig. 4.8: A cylindrical column of air moving adiabatically, conserving potential vorticity.



$$\frac{DC_a}{Dt} = \frac{D}{Dt} (C + fA) = \frac{D}{Dt} (\zeta A + fA) = \frac{D}{Dt} (\zeta + f)A = 0$$

Thus, $(\zeta + f)A$ is conserved following an adiabatic flow.

Now, consider an air column confined between θ_o and $\theta_o + \delta\theta$ by a depth of $\delta p = (p_1 - p_o)$ in a hydrostatic and frictionless (inviscid) atmospheric flow (Fig. 4.8). Based on the conservation of mass,

$$M = \rho \delta V = \rho A \delta z = -\rho A \left(\frac{\delta p}{\rho g} \right) = -\frac{A \delta p}{g}$$

$$\Rightarrow A = -\frac{Mg}{\delta p} = \left(-\frac{Mg}{\delta \theta} \right) \frac{\delta \theta}{\delta p}.$$

Substituting A into (4.11) leads to

$$\left(-\frac{Mg}{\delta \theta} \right) \frac{\delta \theta}{\delta p} (\zeta_\theta + f) = \text{constant} = C_1$$

$$\Rightarrow \left(\frac{M}{\delta \theta} \right) \left(-g \frac{\delta \theta}{\delta p} \right) (\zeta_\theta + f) = C_1$$

Taking the limit of $\delta p \rightarrow 0$, we may define a quantity P as

$$P \equiv \left(-g \frac{\partial \theta}{\partial p} \right) (\zeta_\theta + f) = \frac{C_1 \delta \theta}{M} = \text{a constant} = C.$$

Thus, therefore P is conserved (kept constant) following an adiabatic flow. P is called the Ertel's potential vorticity (or Ertel's PV). In other words, **the Ertel's PV is conserved for an adiabatic, hydrostatic, frictionless flow.** The unit of PV is $K \text{ kg}^{-1} \text{ m}^2 \text{ s}^{-1}$.

- The Ertel PV can be derived more rigorously by applying the Ertel PV Theorem.

[Ertel Potential Vorticity Theorem]

From Stoke's theorem,

$$C_a = \oint \mathbf{V}_a \cdot d\mathbf{l} = \iint_A \boldsymbol{\omega}_a \cdot \mathbf{n} dA \approx (\boldsymbol{\omega}_a \cdot \mathbf{n})A$$

where $\mathbf{n} = \nabla \theta / |\nabla \theta|$ and since $dm = \rho dA dh = \rho dA (\nabla \theta / |\nabla \theta|)$, we have

$$\frac{DC_a}{Dt} = \frac{D}{Dt} [(\boldsymbol{\omega}_a \cdot \mathbf{n})A] = \frac{D}{Dt} \left[(\boldsymbol{\omega}_a \cdot \nabla \theta) \frac{dm}{\rho d\theta} \right] = \left(\frac{dm}{d\theta} \right) \frac{D}{Dt} \left[\frac{\boldsymbol{\omega}_a \cdot \nabla \theta}{\rho} \right] = 0$$

since both dm and $d\theta$ are constants. Thus, for an adiabatic, inviscid fluid flow, we have

$$\frac{D}{Dt} \left[\frac{\boldsymbol{\omega}_a \cdot \nabla \theta}{\rho} \right] = 0 \quad (4.24)$$

The quantity inside the square bracket,

$$\Pi = \frac{\boldsymbol{\omega}_a \cdot \nabla \theta}{\rho} \quad (4.25)$$

is called the **Ertel potential vorticity** which is conserved for an inviscid, adiabatic flow.

An alternative way to derive the conservation of potential vorticity in an inviscid, adiabatic flow is as follow:

- For a moist flow, Ertel's PV may be modified to include the latent heat effect as the **equivalent Ertel's PV**

$$P_e = \frac{\omega \cdot \nabla \theta_e}{\rho},$$

where θ_e is the **equivalent potential temperature**.

$$\theta_e = \theta e^{Lw_s / c_p T}.$$

- **Physical meaning of the Ertel's PV:**

$$P = \frac{\omega_a \cdot \nabla \theta}{\rho} \approx (\zeta_\theta + f) \frac{1}{\rho} \frac{\partial \theta}{\partial z} = \left(\frac{\theta}{g\rho} \right) (\zeta_\theta + f) N^2$$

Which means the PV is proportional to the multiplication of the absolute vorticity and the buoyancy frequency. Also

$$P \approx \frac{\zeta_\theta + f}{\rho \frac{\delta z}{\delta \theta}} = \frac{\text{absolute vorticity}}{\text{effective depth}}$$

- For a homogeneous ($\rho = \text{const}$), incompressible fluid flow, the PV reduces to have

$$P \equiv (\zeta_\theta + f) \left(-g \frac{\partial \theta}{\partial p} \right) \approx \left(\frac{\delta \theta}{\rho} \right) \frac{\zeta_\theta + f}{\delta z} = \text{constant}.$$

This implies that

$$\frac{\zeta_{\theta} + f}{\delta z} = \text{constant}.$$

- **Applications of the PV Conservation**
 - Flow over large-scale mountains

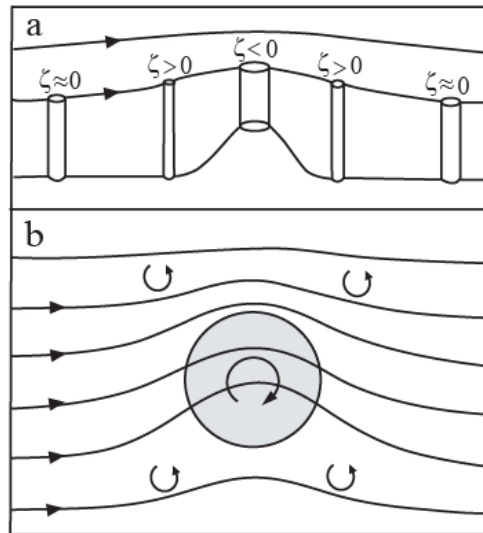


Fig. 5.26: A sketch of a quasi-geostrophic, stratified flow over a circular mountain. (a) The vertical vorticity associated with the deformation of vortex tubes is shown. The solid lines represent trajectories on the vertical cross section through the center of the mountain. (b) The streamline pattern near the surface for the flow associated with (a) as seen from above. ([Lin 2007-Ch.5](#); Adapted from Smith 1979 and Buzzi and Tibaldi 1977)

- Flow over planetary-scale mountains (β effect cannot be ignored)

(a) Westerly flow (From Holton 2004)

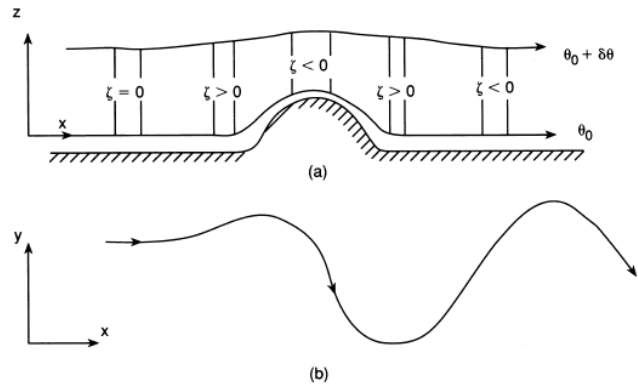


Fig. 4.9 Schematic view of westerly flow over a topographic barrier: (a) the depth of a fluid column as a function of x and (b) the trajectory of a parcel in the (x, y) plane.

(b) Easterly flow

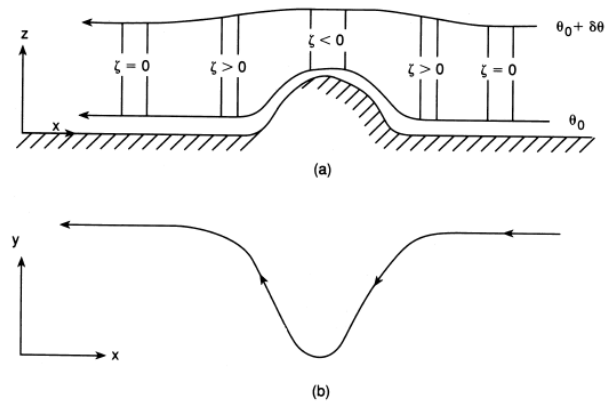
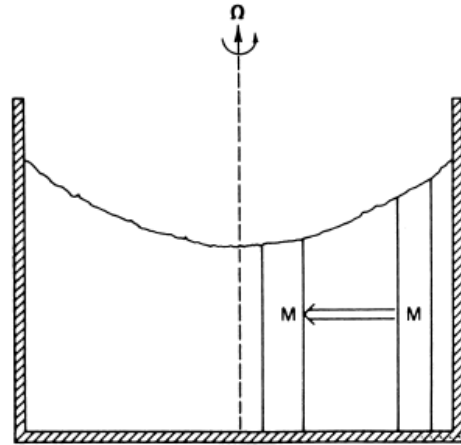


Fig. 4.10 As in Fig. 4.9, but for easterly flow.

- Analogy of depth change of a barotropic fluid and β effect

Fig. 4.11 Dependence of depth on radius in a rotating cylindrical vessel.



An air column moving toward equator (assume $\delta z \sim \text{constant}$)

$\Rightarrow f$ decreases

$\Rightarrow \zeta$ increases.

can be mimicked by a fluid column moving outward in the water tank:

$\Rightarrow \delta z$ increases \Rightarrow vorticity stretching

$\Rightarrow \zeta$ increases (because $(\zeta + f)/\delta z = \text{constant}$)

In other words, the increase of δz produces the same effect as the decrease of f (i.e. the β effect), i.e. increase of ζ . Therefore, the β effect can be simulated by varying the water column depth a tank experiment.

- **Applications of the Conservation of PV Theories**

(a) Idealized fronts passing over elongated mountains

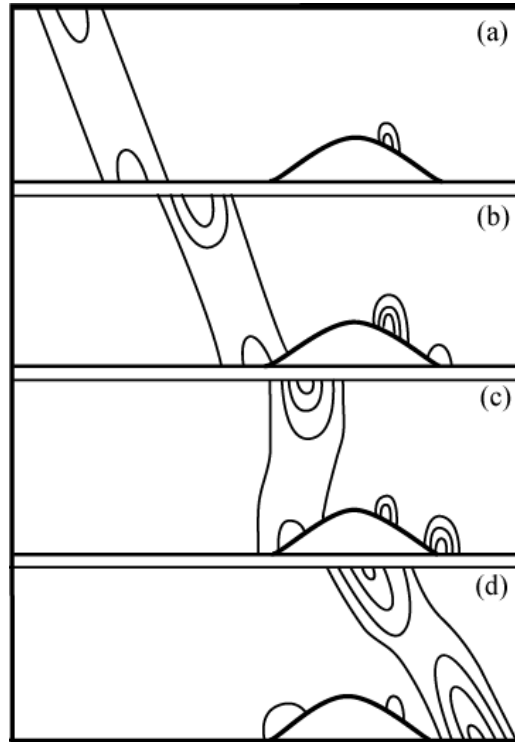


Fig. 6.39: Idealized schematic of a front propagating over a mountain ridge, which indicates the low-level blocking of the front along the windward slope, the development of the lee trough and secondary trough along the lee slope, the separation of the upper-level and lower-level frontal waves, and the coupling of the upper-level frontal wave with the secondary trough in the lee of the mountain. ([Lin 2007-Ch.5](#); Adapted after Dickinson and Knight 1999)

(b) Cold front passing over Alps, CMR, and Appalachians

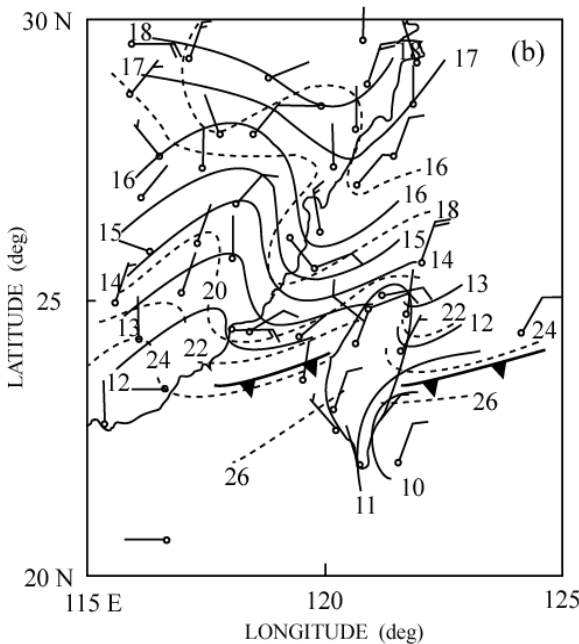
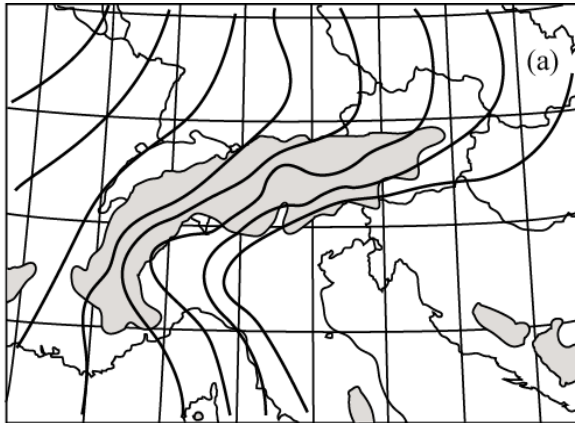


Fig. 6.38: Examples of three-dimensional frontal passage over mesoscale mountains. (a) Schematic of 3-h surface isochrones of a cold front passing over the Alps. (Adapted from Steinacker 1981); and (b) Surface analysis of a Mei-Yu front passing over Taiwan at 1800 UTC 13 May 1987. (Lin 2007-Ch.5; Adapted after Chen and Hui, 1992)

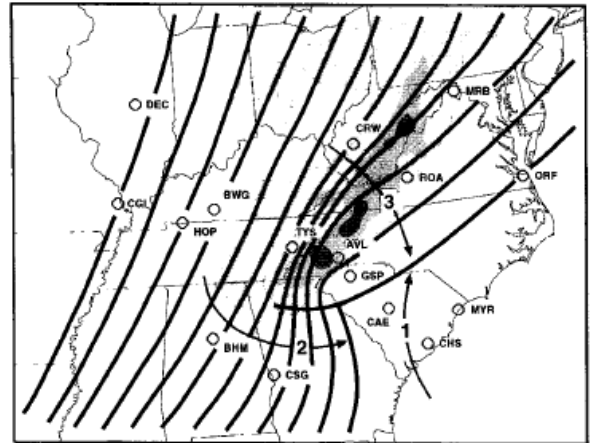


FIG. 5. Schematic showing the horizontal structure of the "average" cold front, every 2 h, as it passes the Appalachians. Analysis was based on the relative times of frontal passage at the plotted stations. Numbered arrows refer to the three airstreams described in the text. Shading represents smoothed topography at 300, 600, and 900 m.

(O'Handley and Bosart, 1996, MWR)

- Lee cyclogenesis over the Alps and Appalachians

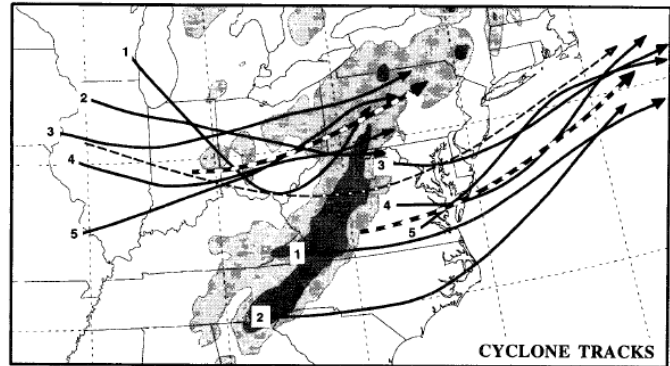
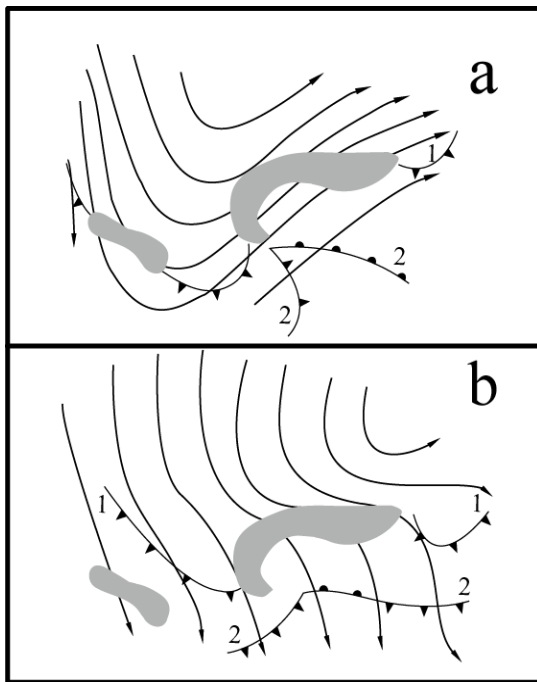


FIG. 10. Tracks of five representative cyclones that exhibited redevelopment across the Appalachians (solid lines). Heavy dashed lines represent approximate "mean" tracks of the primary and secondary cyclones, and the thin dashed line represents an interpolated mean primary cyclone track in the absence of orography. Shading represents smoothed topography at 300 and 600 m.

(O'Handley and Bosart, 1996, MWR)

Fig. 6.31: Schematics of two types of lee cyclogenesis over Alps as proposed by Pichler and Steinacker (1987): (a) Southwesterly upper-level type, and (b) Northwesterly upper-level type. The bold, solid lines indicate the upper-level flow and the surface front is plotted for two consecutive times, as denoted by 1 and 2. ([Lin 2007-Ch.5](#); Adapted after Pichler and Steinacker 1987)

- Lee cyclogenesis over the Rockies

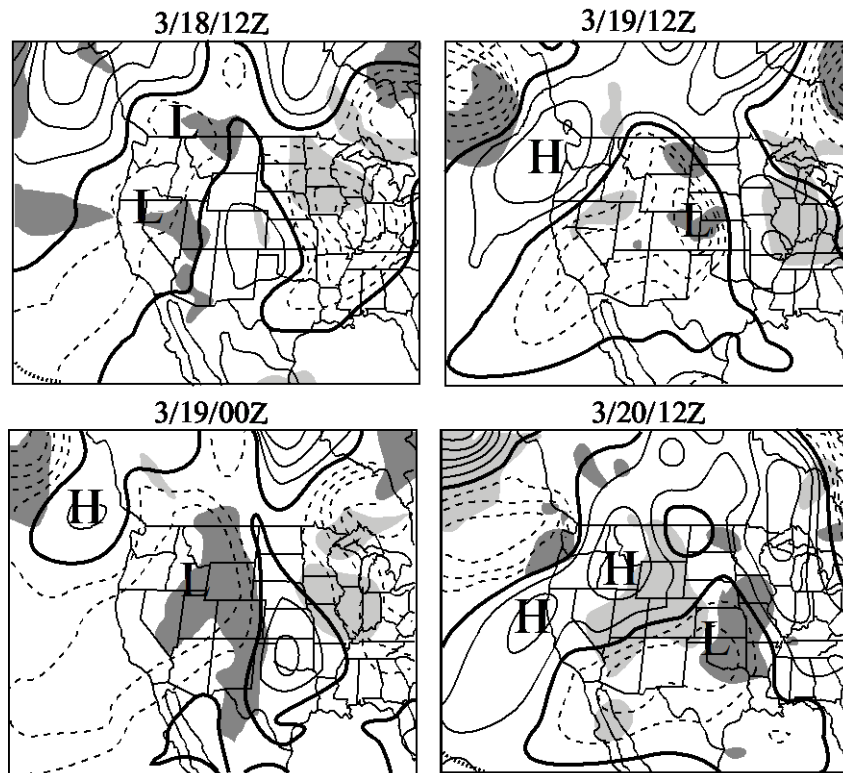


Fig. 5.33: An example of Rockies lee cyclogenesis. Three stages, as summarized in the text, are clearly shown in the perturbation geopotential fields on 860 mb at 12-h intervals from 3/18/12Z (1200 UTC 18 March) to 3/20/12Z 1994. Solid (Dashed) contours denote positive (negative) values, while bold solid contours denote zero geopotential perturbations. Darker (Lighter) shading denotes warm (cold) areas at 900-mb $\theta' \geq 4$ K ($\theta' < 4$ K). ([Lin 2007-Ch.5](#); Adapted after Davis 1997)

- Cyclone track deflection by an elongated mountain

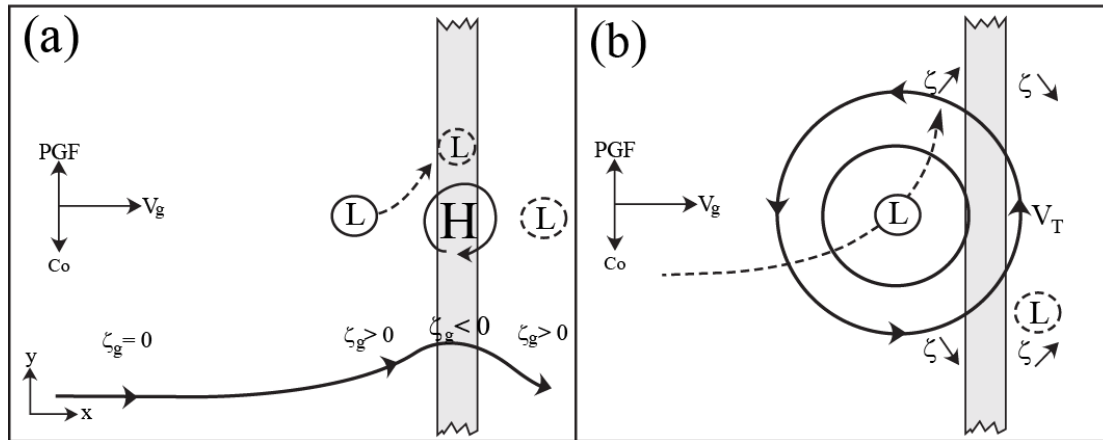


Fig. 5.36: Effects of shallow orography on cyclone track deflection through the turning of (a) the basic flow and (b) outer circulation of the cyclone. The solid-circled L and dash-circled L denote the parent and new cyclones, respectively. The incoming flow is geostrophically balanced. H denotes the mountain-induced high pressure. The lower curve in (a) denotes the trajectory of an upstream air parcel. The cyclone is steered to the northeast by the basic flow velocity V_g . ζ_g is the vertical vorticity associated with the basic flow. In (b), the dashed curve associated with L denotes the cyclone track. The new cyclone forms on the lee due to vorticity stretching associated with the cyclonic circulation that is, in turn, associated with the parent cyclone. V_T is the characteristic tangential wind speed of the parent cyclone, such as the maximum tangential wind (V_{max}). The arrow adjacent to ζ denotes the local vorticity tendency ($\partial\zeta/\partial t$). (From [Lin 2007-Ch.5](#), Cambridge U Press)

- Cyclone track deflection by a finite-length mountain

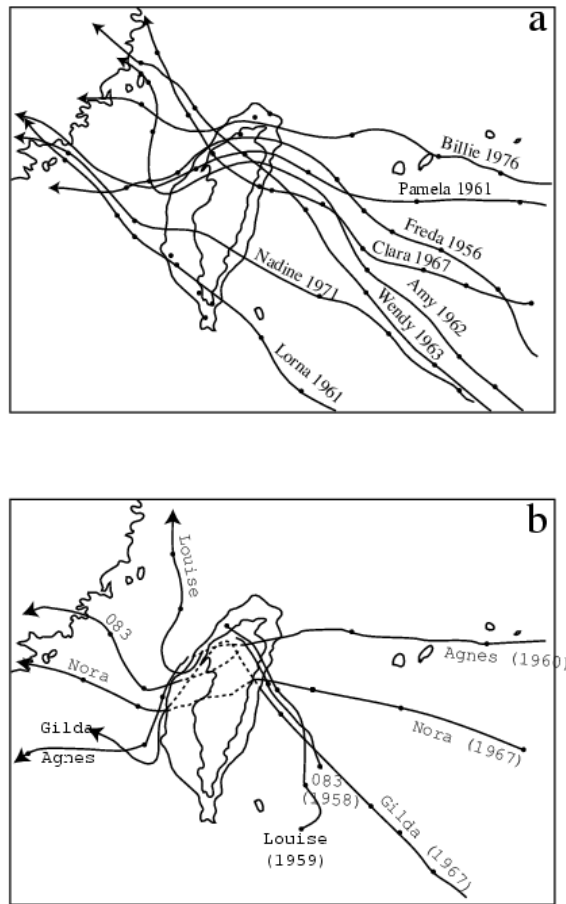
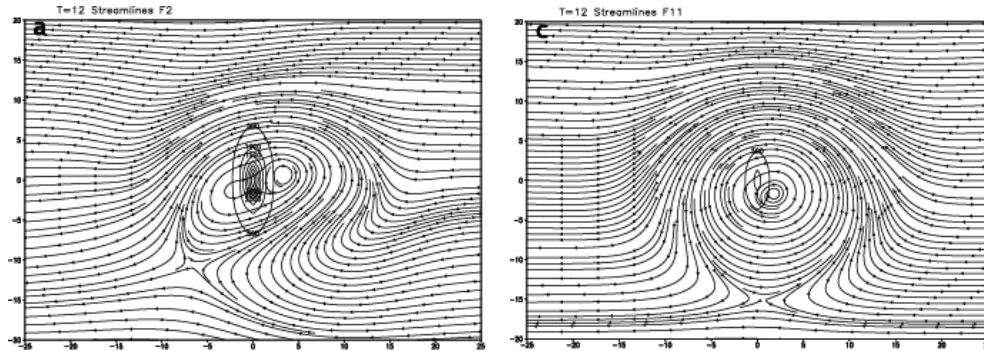
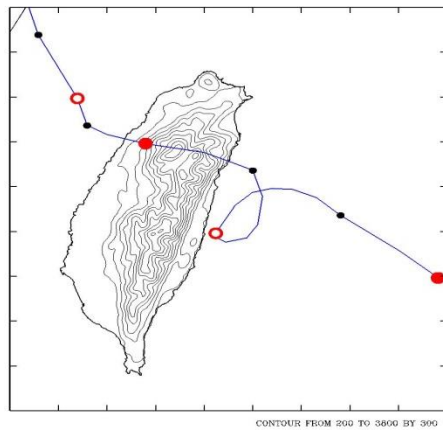


Fig. 5.35: Tropical cyclones traversing the Central Mountain Range (CMR) of Taiwan with (a) continuous tracks, and (b) discontinuous tracks. A cyclone track is defined as discontinuous when the original cyclone (i.e. a low pressure and closed cyclonic circulation) and a lee cyclone simultaneously co-exist. ([Lin 2007-Ch.5](#); Adapted after Wang 1980 and Chang 1982)

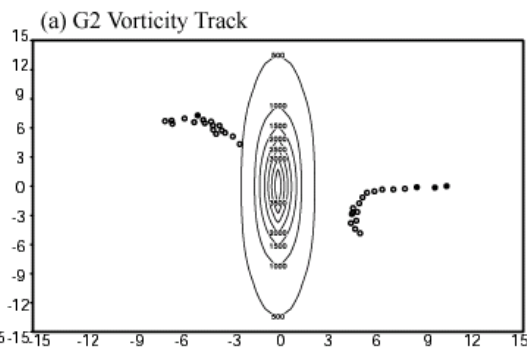
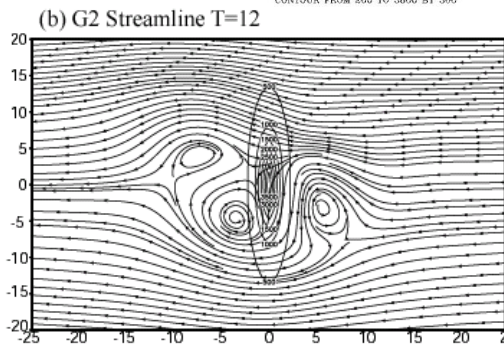
- Flow fields for a cyclone passing over a mesoscale mountain



From Lin et al. (2005 JAS)



Typhoon Haitang (2005)
passing over Taiwan's
CMR (Jian and Wu 2006)



- Pressure, vorticity, and PV fields

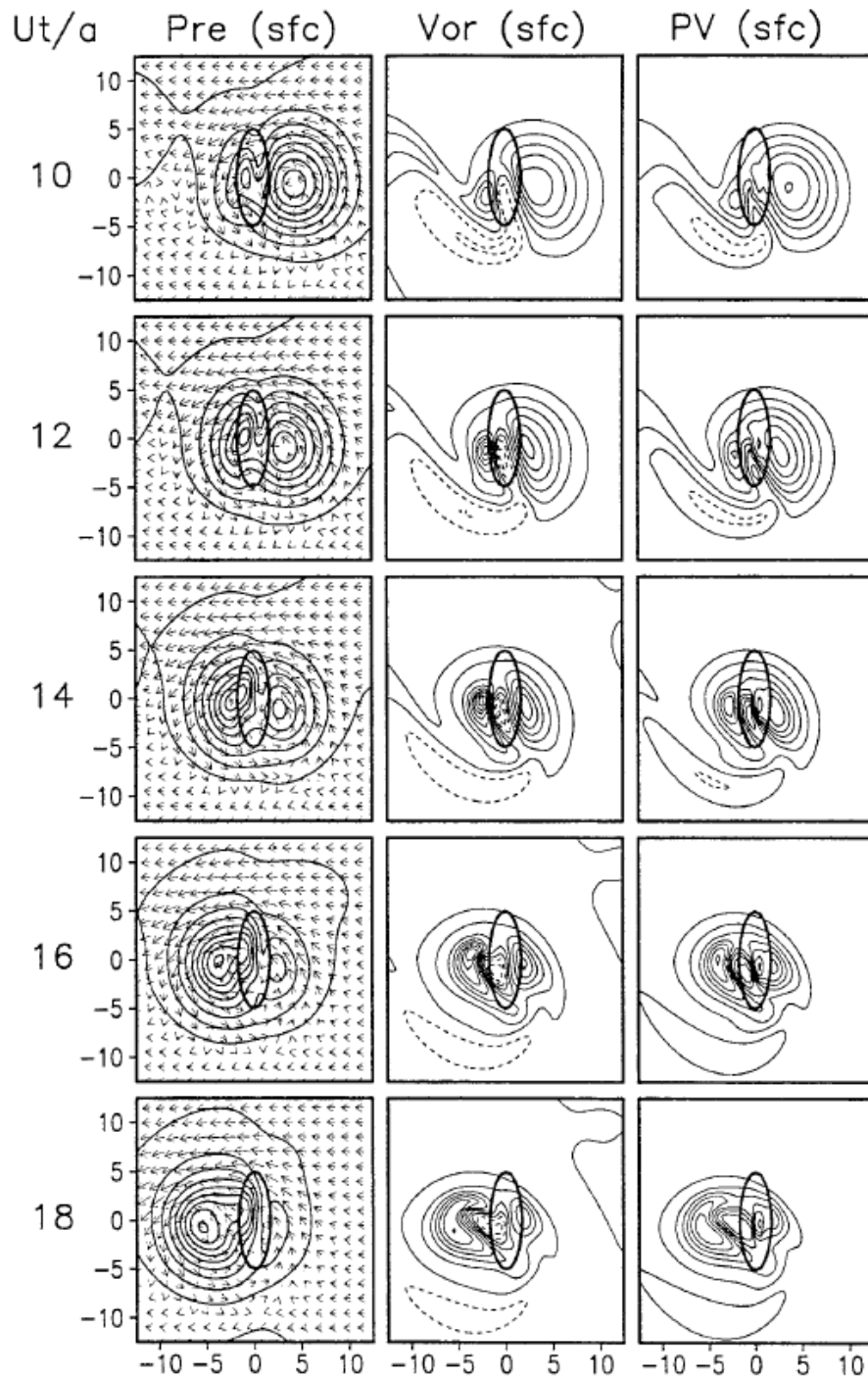


FIG. 11. Same as Fig. 7 except for a propagating cyclone embedded in an easterly flow over an idealized mountain range.

From Lin et al. (1999 JAS)

- Mechanism for cyclone track deflection over a mesoscale mountain

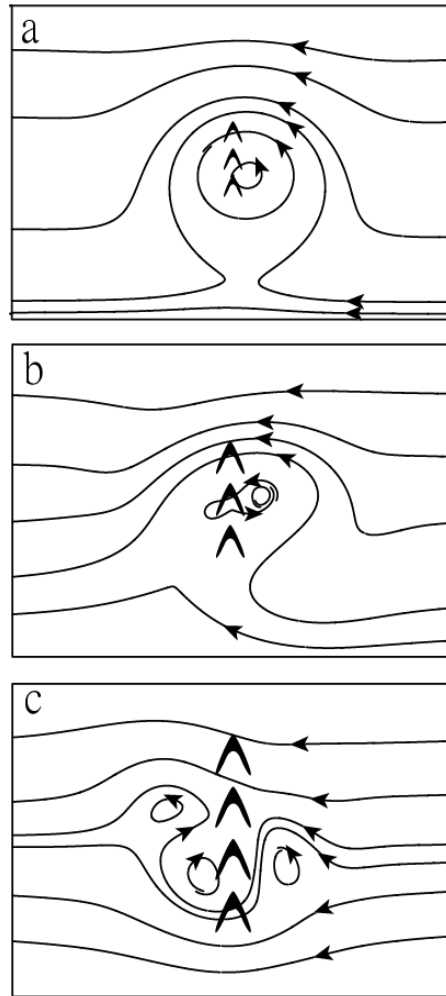
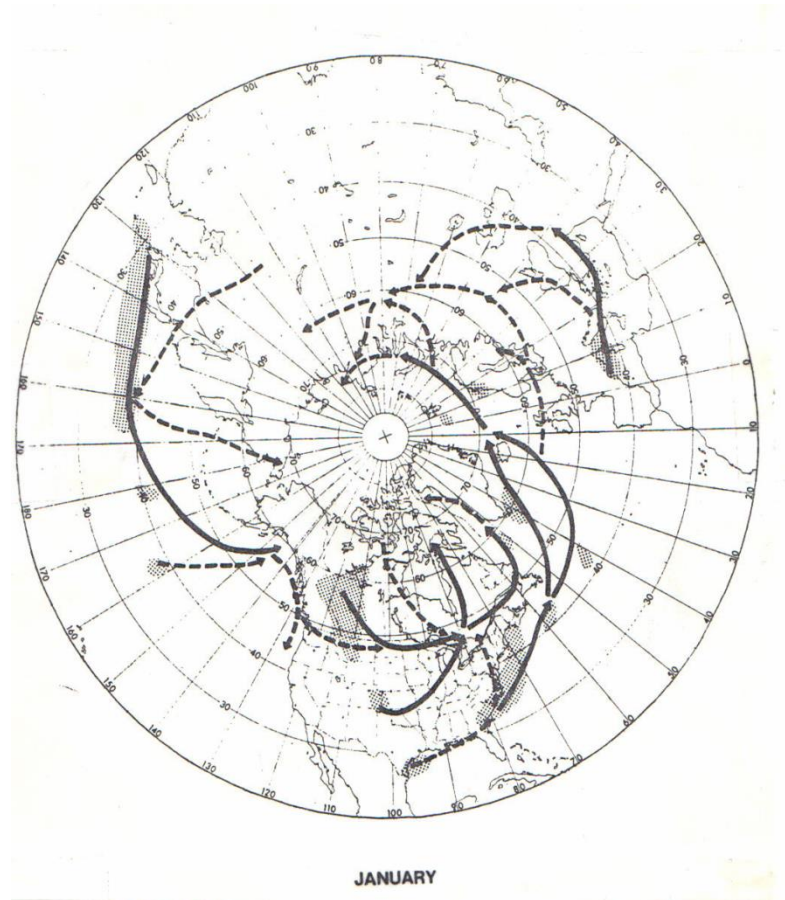


Fig. 6.37: A conceptual model depicting three different responses of a westward propagating cyclone to orographic forcing: (a) weak blocking, (b) moderate blocking, and (c) strong blocking. The strength of blocking may be controlled by some nondimensional parameters, such as V_{\max}/Nh and R/L_y .

([Lin 2007-Ch.5](#); After Lin et al. 2005)

- Influence on storm tracks



Two major regions of cyclogenesis (wherever has strong forcing):

1. Lee side of major mountain ranges (e.g., Rockies, Alps, Andes, etc.) and
2. Across a region with strong differential heating [e.g., Gulf Stream (induced Atmospheric Bomb), [Kuroshio](#)].